Proceedings of the Sixth International Conference on
Railway Technology: Research, Development and Maintenance
Edited by: J. Pombo
Civil-Comp Conferences, Volume 7, Paper 4.12
Civil-Comp Press, Edinburgh, United Kingdom, 2024
ISSN: 2753-3239, doi: 10.4203/ccc.7.4.12

Review of Perspectives on Pantograph-Catenary Interaction Research for High-Speed Railways Operating at 400 km/h and Above

Y. Song

School of Electrical Engineering, Southwest Jiaotong University
Chengdu, China

Abstract

In this survey paper, we comprehensively examine the ongoing research concerning the interaction between pantographs and catenaries, a vital aspect in ensuring uninterrupted electricity supply to trains. Future perspectives for future studies to ensure satisfactory performance at 400 km/h and above are preliminarily explored. Initially, this paper provides an overview of the current design and assessment system. A systematic survey on the numerical modelling of pantograph-catenary interaction is conducted. The applicability of current assessment quantities to speeds of 400 km/h and above is preliminarily investigated with a numerical model. The potential of optimising parameters for improving interaction performance is also explored at this speed level. The paper further reviews and preliminarily analyses the effects of common disturbances, such as geometric deviation on the pantograph-catenary interaction performance at 400 km/h and above. Overall, this paper offers insights into the current state of research on pantograph-catenary interaction for high-speed railways and proposes future directions for improving the system to ensure optimal performance at speeds of 400 km/h and above.

Keywords: high-speed railway, pantograph-catenary system, 400 km/h and above, current collection quality, parameter optimisation, numerical modelling.

1 Introduction

Over the past decade, there has been a remarkable expansion of high-speed rail networks across the world. These networks offer a fast, comfortable, robust and

environmentally friendly travel option. The modern high-speed railway is defined by its commercial speed of over 250 km/h, which surpasses the conventional passenger dedicated lines of 200 km/h. In many high-speed networks today, a commercial speed of over 300 km/h is common, with maximum speeds in Japan, France, Spain and Germany reaching 320km/h, 320km/h, 310km/h and 300 km/h, respectively. The Beijing-Shanghai high-speed railway in China holds the record for the fastest commercial speed at 350 km/h.

In many countries, the next generation of high-speed railways aiming for even higher speeds is currently being developed. For instance, the HS2 project in the UK aims to build a high-speed line with a design speed of 360 km/h [1], while in China, the Chengdu-Chongqing high-speed railway with a design speed of 400 km/h is currently under construction [2]. The alfa-X Shinkansen in Japan can travel up to 400 km/h and has already begun testing [3], and in Russia, the next generation of a high-speed train with speeds up to 400 km/h is being developed by Russian Railway and Sinara [4]. All of these examples demonstrate the importance of accelerating fundamental studies of high-speed technology, even at the speed class of 400 km/h and above. Different from the solution of maglev [5], [6], the electric train still replies on an electric contact to collect current. One of the key technical challenges is to keep a continuous transmission of power to the high-speed train, which relies heavily on the interaction performance of the pantograph-catenary [7], [8]. Various studies have recognised the pantograph-catenary system as the most vulnerable part of the traction power system [9]. As a result, there has been an ever-increasing focus on the service performance of the pantograph-catenary system from both the industrial and academic communities [10].

The public transport industry is forging ahead to meet all the emerging challenges of developing the economy and society. The speed of 400 km/h is the target of the next generation of high-speed rail being developed in many countries. However, operating at 400km/h poses unprecedented challenges to pantograph-catenary interaction stability and service safety. The sliding speed of the pantograph is close to the limit of catenary wave speed, and the pantograph-catenary coupling vibration becomes extremely intense. The contact between them tends to be rigid, and the tolerance for irregularities in contact surfaces is stricter. All these changes lead to a more complicated dynamic behaviour of the pantograph-catenary and more stringent design and assessment standards. Currently, there is no construction or operation experience or technical standards for high-speed railways at the speed of 400 km/h and above. Thus, it is necessary to carry out research on the interaction performance of pantograph-catenary at 400 km/h and above and update the technical standards for pantograph-catenary system design, equipment manufacturing, and operation & maintenance at this speed level.

Motivated by the goal of developing the next generation of high-speed rail, it tends to be essential to comprehensively review the advanced and updated research outputs in the field of pantograph-catenary interaction. In combination with mature techniques at a speed of lower than 350 km/h, the preliminary investigation is also performed in this paper to identify perspectives on the research of pantograph-catenary at 400 km/h and above. The schematics of this review paper are shown in Figure 2. The main contribution of this work can be summarised as follows.

- The first emphasis of this paper is on a systematic survey of the numerical modelling technique used for the pantograph-catenary system and preliminarily investigates the application of assessment quantities to the speed of 400 km/h and above.
- The second aim is to review the current design and assessment standard framework. It is fundamental to understand the quantitative representation of the current collection quality and operation safety of the pantograph-catenary system.
- The third attention is, by preliminarily mining the potential of parameters' optimisation in improving the interaction performance to identify the challenges in designing the pantograph-catenary system at 400 km/h.
- The fourth attempt is motivated by practical applications to summarise and preliminarily investigate the effect of common disturbances (such as the geometric deviation and aerodynamics) on the pantograph-catenary interaction performance at 400 km/h and above.

2 Numerical Modelling at 400 km/h

In this subsection, we present a classic numerical model based on ANCF, which has already been demonstrated to have an acceptable numerical accuracy in describing structural nonlinearity [11]. The model of catenary with ANCF is described here. Figure 1 shows an ANCF beam element representing the contact, messenger, and stitch wires. A similar cable element without bending degrees of freedom is used to model the dropper and steady arm. Claws and clamps in the connection points are assumed as lumped masses attached to the wire. Considering an ANCF beam element with two nodes, I and J, the nodal degree of freedom (DOF) vector that contains the displacements and the gradients is defined as

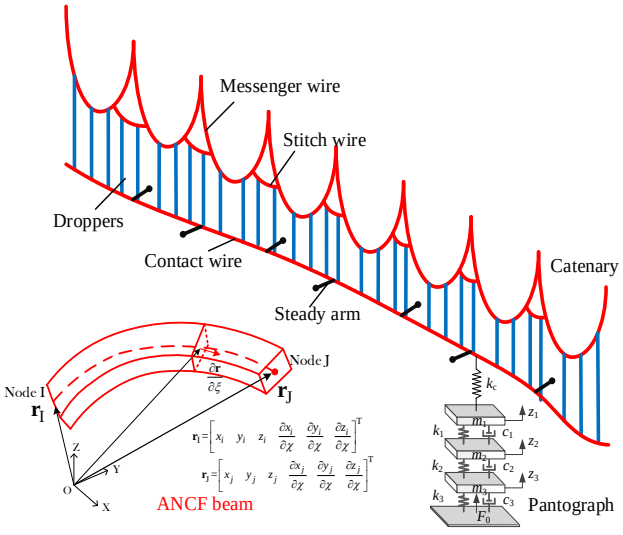

Figure 1. Catenary model based on ANCF beam and cable elements. Red lines denote the ANCF beam element, and blue lines denote the ANCF cable element

$$\mathbf{e}=\left[\begin{array}{cccccccccccc} x_i & y_i & z_i & \dfrac{\partial x_i}{\partial \chi} & \dfrac{\partial y_i}{\partial \chi} & \dfrac{\partial z_i}{\partial \chi} & x_j & y_j & z_j & \dfrac{\partial x_j}{\partial \chi} & \dfrac{\partial y_j}{\partial \chi} & \dfrac{\partial z_j}{\partial \chi} \end{array}\right]^{\mathrm{T}} \quad 1)$$

where χ is the local coordinate along the beam ranging from 0 to the undeformed element length l_0. The global position vector $\mathbf{r}$ can be expressed by

$$\mathbf{r} = \mathbf{S}\mathbf{e} \tag{2}$$

where $\mathbf{S}$ is a classical shape function matrix used in the finite element method [11]. The strain energy is calculated by the summation of the contributions of axial and bending deformations, which is expressed as

$$U = \frac{1}{2}\int_0^{L_0} (EA\varepsilon_l^2 + EI\kappa^2) d\chi \tag{3}$$

where E is the Elastic modulus, A is the cross-sectional area, I is the moment of inertia. The axial strain ε_l and the curvature κ can be expressed by [12]

$$\varepsilon_l = \frac{1}{2}\left(\frac{\partial \mathbf{r}}{\partial \chi}^{\mathrm{T}} \frac{\partial \mathbf{r}}{\partial \chi} - 1\right) = \frac{1}{2}\left(\mathbf{e}^{\mathrm{T}} \frac{\partial \mathbf{S}}{\partial \chi}^{\mathrm{T}} \frac{\partial \mathbf{S}}{\partial \chi}\mathbf{e} - 1\right) \tag{4}$$

$$\kappa = \left|\frac{\partial^2 \mathbf{r}}{\partial \chi^2}\right| = \sqrt{\mathbf{e}^{\mathrm{T}} \frac{\partial^2 \mathbf{S}}{\partial \chi^2}^{\mathrm{T}} \frac{\partial^2 \mathbf{S}}{\partial \chi^2}\mathbf{e}} \tag{5}$$

The generalised elastic forces $\mathbf{Q}$ can be defined as

$$\mathbf{Q} = \frac{\partial U}{\partial \mathbf{e}}^{\mathrm{T}} = \mathbf{K}_{\mathrm{e}}\mathbf{e} \tag{6}$$

Thus, the matrix $\mathbf{K}_{\mathrm{e}}$ relevant to the absolute coordinate can be obtained. But we prefer to use the tangent stiffness matrix that can iteratively calculate the incremental nodal DOF vector $\Delta\mathbf{e}$ and the incremental unstrained length Δl_0 in both the shape-finding and dynamic simulation procedures. The tangent stiffness matrices $\mathbf{K}_{\mathrm{T}}$ and $\mathbf{K}_{\mathrm{L}}$ can be obtained by the derivative of Eq. (6) with respect to $\mathbf{e}$ and l_0 as

$$\Delta\mathbf{F} = \frac{\partial \mathbf{Q}}{\partial \mathbf{e}}\Delta\mathbf{e} + \frac{\partial \mathbf{Q}}{\partial L_0}\Delta L_0 = \mathbf{K}_{\mathrm{T}}\Delta\mathbf{e} + \mathbf{K}_{\mathrm{L}}\Delta L_0 \tag{7}$$

Eq. (7) can be used to calculate the incremental DOF vector and unstrained length. After obtaining the initial configuration, the equation of motion for the catenary system can be obtained by introducing a consistent mass matrix $\mathbf{M}_{\mathrm{C}}^{\mathrm{G}}$ and Raleigh damping matrix $\mathbf{C}_{\mathrm{C}}^{\mathrm{G}}$.

$$\mathbf{M}_{\mathrm{C}}^{\mathrm{G}}\ddot{\mathbf{U}}_{\mathrm{C}}(t) + \mathbf{C}_{\mathrm{C}}^{\mathrm{G}}\dot{\mathbf{U}}_{\mathrm{C}}(t) + \mathbf{K}_{\mathrm{C}}^{\mathrm{G}}(t)\mathbf{U}_{\mathrm{C}}(t) = \mathbf{F}_{\mathrm{C}}^{\mathrm{G}}(t) \tag{8}$$

where $\mathbf{K}_{\mathrm{C}}^{\mathrm{G}}$ is the stiffness matrix of the catenary system, respectively. The damping coefficients identified from a realistic China high-speed railway catenary [13] are adopted here to generate the damping matrix $\mathbf{C}_{\mathrm{C}}^{\mathrm{G}}$. The vector $\mathbf{U}_{\mathrm{C}}(t)$ is the global DOF vector, and $\mathbf{F}_{\mathrm{C}}^{\mathrm{G}}(t)$ on the right hand is the external force vector. In the dynamic simulation of pantograph-catenary interaction, the iteration is performed in each time step. The displacements of the pantograph and the catenary are calculated by exerting the contact force on both the catenary model and pantograph model, respectively. Through the penetration assumption as reported in [14], the contact force is updated according to the uplifts of the contact wire and the pantograph head. In the first time step, the pantograph is lifted to contact with the contact wire, and calculate the static contact force and the initial displacement. A Newmark integration scheme is adopted to solve Eq. (8). The stiffness matrix $\mathbf{K}^{\mathrm{G}}(t)$ is updated according to the catenary

deformation in each time step to fully describe the nonlinearity of messenger/contact wires and the slackness of droppers.

In order to validate the numerical accuracy of the present model at 400 km/h or above, the measurement data from field tests conducted by China Railway Group on the Fuzhou-Xiamen high-speed line in June 2023 (as shown in Figure 2) is obtained. The pantograph used in this test is a special one newly manufactured by CRRC (China Railway Rolling Stock Corporation) special for the CRH 450 high-speed train. Taking the design data and the static measurement data of two tensile sections of the catenary, the numerical simulation is performed at the same speed as the field test. Taking the design data of two tensile sections of the catenary, the numerical simulation is performed at the same speed as the field test. The comparison of contact force statistics between the simulation and field test is presented in Table 1. Note that the contact forces are all filtered within the frequency range of interest, 0-20 Hz. It can be seen that all simulation contact force statistics show a significant agreement with the measurement data. Particularly, the maximum error of the contact force standard deviation at 400.7 km/h is only 5.42%.

(a)

(b) (c)

Figure 2. CRH 450 field test: (a) test field; (b) maximum test speed; (c) Inspection train

Table 1. Comparison of contact force statistics between simulation and field test

Speed [km/h]	Maximum [N]		Minimum [N]		Mean [N]		Standard deviation [N]		
	Meas.	Sim.	Meas.	Sim.	Meas.	Sim.	Meas.	Sim.	Error (%)
351.3	271	266.93	114	77.082	185.5	185.30	28.1	27.27	-2.95
400.7	353	354.94	134	128.03	219.2	221.23	32.3	34.05	5.42
413.6	356	336.10	136	139.82	232.6	233.27	33.1	32.64	-1.38

In terms of the contact force statistics filtered within 0-20 Hz, the current numerical technique can generally satisfy the numerical accuracy at the speed of 400 km/h and above. However, with the increase of speed, the high-frequency behaviours are more critical to reflect the current collection quality and operational safety. The contact model between the pantograph and contact wire used in previous research is oversimplified to reflect the high-frequency behaviours. Particularly, an advanced contact model integrated with the friction between two contact surfaces can describe some abnormal behaviours that may happen at super high speed. As reported in [15], the friction-induced, self-excited vibration of a pantograph-catenary may be triggered

at a given speed and cause the instability of the pantograph. The lumped pantograph model used in previous studies is too simple to describe high-order modes of the pantograph, which are related to the contact loss and arcing happening at high frequencies [16]. A fully finite element model is preferred to exhibit the geometry and flexibility of key components of the pantograph, as illustrated in Figure 7. However, a detailed model arouses the issue of tremendous computational cost, which relies on the upgrade of the numerical integration scheme. One of the potential solutions is the combination of multibody and finite element integration methods, as reported in [17]. The semi-implicit coupling technique is presented in this work to reduce the computational effort by using Jacobian information only with respect to the coupling variables, which can achieve a very time-efficient integration for the complex dynamics system. Other solutions rely on the development of neural network-based integration algorithms, as reported in [18], which train a surrogate model to calculate the results at a given time instant using the information from previous time steps.

3 Design and Assessment System of Pantograph-Catenary

In this section, the interaction performance at the speed of 400 km/h is preliminarily analysed with the abovementioned pantograph-catenary model. As specified in En 50367 [19], the frequency of interest of 0-20 Hz is adopted in the analysis. Figure 3 presents the contact force statistics, including the standard deviation and maximum and minimum values at the speeds of 320 km/h, 360 km/h and 400 km/h. A sharp increase in all the contact force statistics can be observed when the speed increases from 360 km/h to 400 km/h. Particularly, the contact force standard deviation increases by 34.86%, which indicates a significant deterioration of the current collection quality. It is normally assumed that the contact force follows the Gaussian distribution [20], and the three-sigma rule that corresponds to a 95% confidence level is widely used to evaluate the fluctuation margin of the contact force. Figure 4 presents the contact force margin with a 95% confidence level at the speeds of 320 km/h, 360 km/h and 400 km/h. The current standard requires the maximum contact force to be lower than 350 N, and the minimum contact force should be positive to avoid potential contact loss. It is observed from Figure 4 that even though the speed reaches up to 400 km/h, the contact force margin is still within the acceptance range, which indicates the feasibility of the speed upgrades in existing high-speed lines for trains with a single pantograph. The spectrum of the contact force at three speeds is presented in Figure 5. It is seen that the previous frequency of interest covers almost all the primary frequency components at the speed of 320 km/h. However, some frequency components are outside of 0-20Hz when the speed reaches 360 km/h and 400 km/h. The previous frequency range of interest is desired to be improved to reflect the necessary dynamic behaviours at a higher speed. But this improvement should also take the limitation and economy of measurement accuracy into account. Here, to fulfil the subsequent analysis, we update the frequency range of interest to 0-25 Hz to cover the significant frequency components at 360 km/h and 400 km/h. It should be noted that the frequency range of interest for 400 km/h should be further analysed with more strict research in the future. The suggested frequency range, 0-25 Hz, is only to facilitate the preliminary analysis in this review paper.

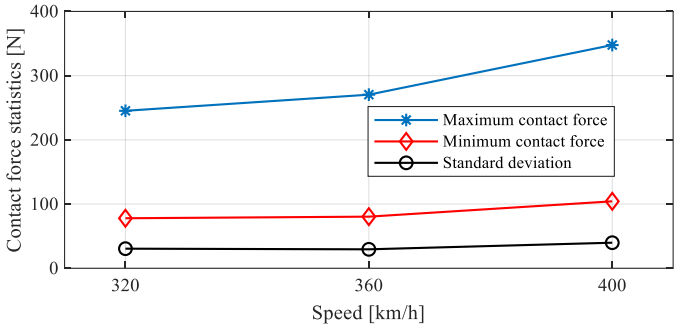

Figure 3. Contact force statistics at 320 km/h, 360 km/h and 400 km/h

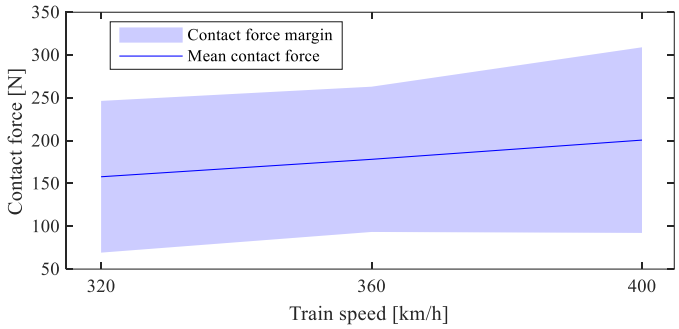

Figure 4. Contact force margins with 95% confidence level at 320 km/h, 360 km/h and 400 km/h

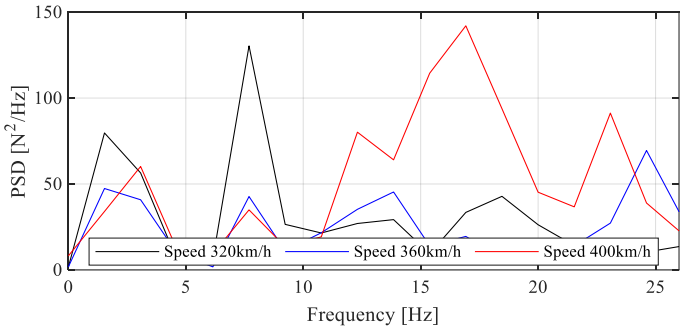

Figure 5. PSDs of contact force at 320 km/h, 360 km/h and 400 km/h

It is a common strategy to equip the high-speed train with double pantographs to enhance the transport capacity [21]. It is challenging to maintain a good current collection quality for the trailing pantograph, as it is disturbed by the mechanical wave and contact wire vibration caused by the leading pantograph [22]. The basic understanding of the deterioration of the trailing pantograph's current collection quality is the resonance caused by the match between the pantograph's interval and the catenary mode [23]. Here, the simulations of the double pantographs-catenary interaction are performed at the speed level of 400 km/h. The contact force margins of leading and trailing pantographs filtered within 0-20 Hz at 320 km/h, 360 km/h and 400 km/h are presented in Figure 6. It can be seen that the trailing pantograph's performance is much worse than the leading one's. When the speed reaches 400 km/h, the contact force margin will be larger than the contact force maximum limit, 350 N. The lowest boundary is almost outside of the minimum limit of 0 N. Taking

the suggested frequency range of interest, 0-25 Hz, the contact force margins of leading and trailing pantographs with 95% confidence level at 320 km/h, 360 km/h and 400 km/h are presented in Figure 7. It is obvious that the contact force margin is outside of both the maximum and minimum limits of the acceptance range at 400 km/h.

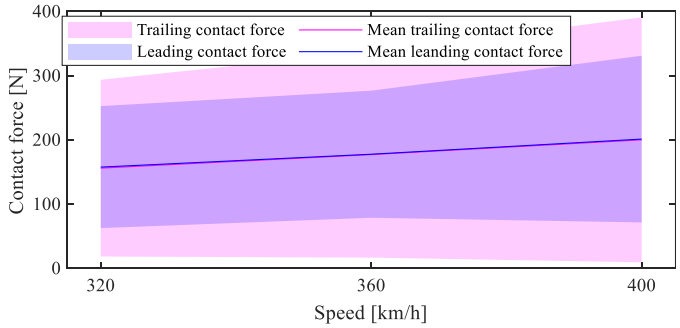

Figure 6. Contact force margins of leading and trailing pantographs filtered within 0-20 Hz with 95% confidence level at 320 km/h, 360 km/h and 400 km/h

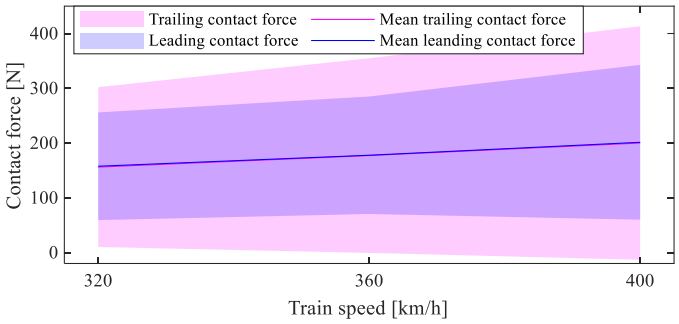

Figure 7. Contact force margins of leading and trailing pantographs filtered within 0-25 Hz with 95% confidence level at 320 km/h, 360 km/h and 400 km/h

The above analysis results indicate that the biggest challenge of developing the pantograph-catenary at 400 km/h is to ensure the trailing pantograph's interaction performance. The literature review and preliminary analysis have pointed out that the current modelling technique is sufficient for the pantograph-catenary system at the speed level of 380 km/h with acceptable numerical accuracy of reproducing the interaction behaviours within 0-20 Hz. More experimental data should be provided to validate the numerical model with more details, such as the overlap section and high-frequency behaviours at higher speeds. The necessity of including more details related to the high-frequency behaviours, such as the pantograph flexibility, short-wavelength wavelength, wear on the strip and contact wire and variability of parameters, should be further investigated.

The current assessment standard specifies the frequency range of interest for the contact force to be 0-20 Hz. The main frequency components will be outside of this specific frequency range with the increase of train speed up to 400 km/h and above. The increase of this frequency range requires the improvement of both the numerical and field test techniques. Combined with the maintenance demand, an appropriate frequency range of interest should be updated with the speed upgrade. The suggested

frequency range, 0-25 Hz in this preliminary analysis should be further assessed to check if it is sufficient to reflect the current collection quality.

4 Parameters' Selection of Catenary For 400 km/h

Wave propagation plays an important role in affecting the system's stability with various backgrounds [24], [25]. Generally, the effects of waves on contact quality of pantograph-catenary can be seen from two sources. One is the limitation to the maximum speed. The wave speed [26], as described in Eq. (9), is the maximum limit of the train speed.

$$c_{\mathrm{cw}} = \sqrt{\frac{T_{\mathrm{cw}}}{\rho_{\mathrm{cw}}}} \tag{9}$$

in which T_{cw} is the contact wire tension and ρ_{cw} is the linear density of the contact wire. It can be seen that the wave speed is a quantity used for determining the contact wire tension. Using the above-mentioned pantograph-catenary model, the effect of the wave speed on the current collection quality is analysed. The contact wire tension is increased from 30 kN to 36 kN with an interval of 2 kN. Figure 8 presents the contact force margins of leading and trailing pantographs filtered within 0-25 Hz with a 95% confidence level at different contact wire levels. The corresponding wave speed increases from 538.25 km/h to 589.63 km/h with the increase of T_{cw} from 30 kN to 36 kN. It is seen that the increase of T_{cw} significantly reduces the contact force fluctuation range. Particularly, the lower boundary of the contact force margin becomes positive when T_{cw} increases more than 32 kN. Thus, the increase of tension is always the effective measure to increase the current collection quality, even at 400 km/h. But the tension cannot be infinitely improved as it is restricted by the material yield limit. Thus, the improvement of the interaction performance at a given T_{cw} class is necessary to enable a faster train.

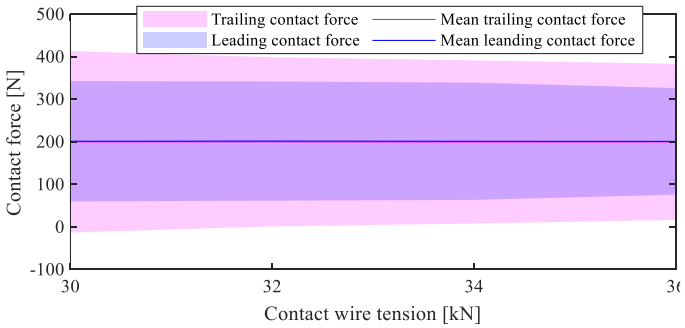

Figure 8. Contact force margins of leading and trailing pantographs filtered within 0-25 Hz with 95% confidence level at the contact wire tension levels of 30-36 kN

The other effect of the wave motion is the disturbance from the reflection wave to the pantograph. Particularly, when the wave comes across a dropper, the reflected wave by the lumped stiffness or mass may have a negative effect on the pantograph-catenary interaction. The intensity of the reflection wave can be quantified by the reflection coefficient C_{r}, which can be expressed by [27]

$$C_{\mathrm{r}} = \frac{1}{1+\sqrt{\frac{T_{\mathrm{cw}}\rho_{\mathrm{cw}}}{T_{\mathrm{mw}}\rho_{\mathrm{mw}}}}} \tag{10}$$

in which T_{mw} is the messenger wire tension, and ρ_{mw} is the linear density of the messenger wire. Due to the Doppler effect, the wave is compressed in front of the fast-moving pantograph, and the wavelength becomes shorter. The Doppler coefficient α used for quantifying the Doppler effect can be written by [28]

$$\alpha = \frac{c_{\mathrm{cw}} - v}{c_{\mathrm{cw}} + v} \tag{11}$$

The Doppler effect can amplify the negative effect of reflection waves on the pantograph's contact quality. Normally, the amplification coefficient γ calculated by the ratio between the reflection and Doppler coefficients is used to evaluate this amplification effect

$$\gamma = \frac{C_{\mathrm{r}}}{\alpha} \tag{12}$$

The reflection and amplification coefficients should be lowered to reduce the effect of reflection waves on the interaction performance. According to industrial experience [29], the reflection coefficient should be around 0.4, and the amplification coefficient should be within 0.2-0.4 to ensure acceptable performance. The amplification and reflection coefficients are used to determine the messenger wire tension. Taking the catenary system analysed above as an example, the reflection and amplification coefficients versus the messenger wire tension are shown in Figure 9. Considering the current messenger wire tension is 21 kN, both coefficients are around 0.4, which are acceptable according to the current specification. Using the numerical model, T_{mw} changes from 15 kN to 29 kN with an interval of 2 kN to perform the numerical simulation. Figure 10 presents the resulting contact force margins of leading and trailing pantographs filtered within 0-25 Hz with a 95% confidence level at T_{mw} of 15-29 kN. The decrease of T_{mw} does not reduce the contact force fluctuation as expected. Particularly, the contact force of the leading pantograph slightly decreases as the increase of T_{mw}. Only the performance of T_{mw} = 27 kN is better than that of T_{mw} = 29 kN. For the trailing pantograph, it is difficult to observe any patterns on how the change of T_{mw} affects the contact force. The preliminary analysis results indicate that the performance no longer shows a significant increase with the decline of the reflection or amplification coefficients at 400 km/h. Therefore, the design of catenary parameters does not have to strictly follow the previous design criterion. Maybe the optimisation procedure is preferred to obtain the optimal design strategy of the catenary system at 400 km/h.

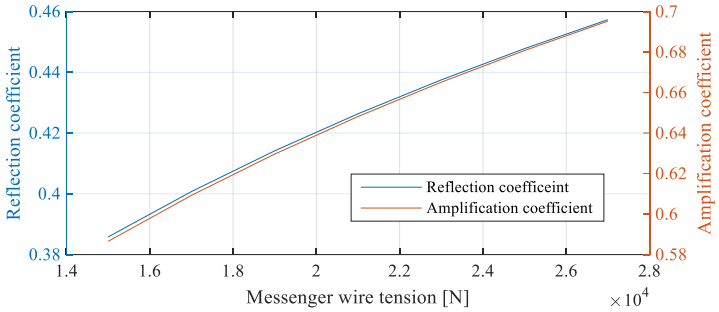

Figure 9. Reflection and amplification coefficients versus messenger wire tension

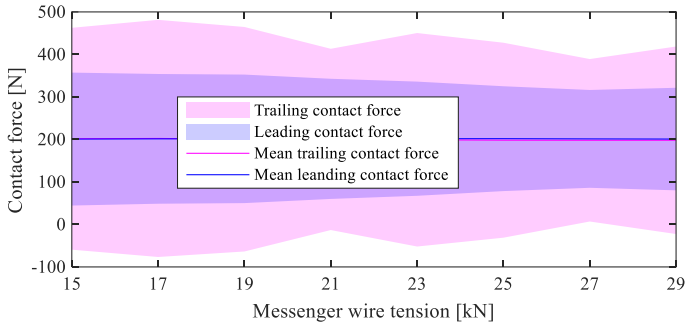

Figure 10. Contact force margins of leading and trailing pantographs filtered within 0-25 Hz with 95% confidence level at the messenger wire tension levels of 15-29 kN

Due to the complexity of the pantograph-catenary system, the parametric optimisation is preferred to achieve optimal interaction performance with certain constraints regardless of the design criterion. The sensitivity analysis of the main parameters of the contact quality has been reported in [30], [31]. The analysis results generally indicate the potential of further parametric optimisation in improving the current collection quality at a specific range of T_{cw}. Implementing the optimisation approach does not require the revelation of the complex dynamic behaviours and the wave propagation property. The optimisation algorithm can automatically find the best parameter setting to minimise contact force fluctuation [32]. In [33], a genetic geometric optimisation approach is implemented to reduce the contact force standard deviation by updating the geometric parameters. The optimisation of a pantograph can be found in [34]. The objective of the optimisation is also to reduce the contact force standard deviation. A similar work is presented in [35] to optimise the pantograph at different train speeds. Considering both the pantograph and catenary systems, a neural network-based optimisation approach is implemented to improve the current collection quality of the high-speed pantograph catenary system [36]. The results indicate that an over 30% reduction in contact force standard deviation can be achieved at a given tension class.

The maximum speed considered in the above optimisation analysis is no more than 360 km/h. Considering the increasing complexity of the pantograph-catenary dynamics, it may be difficult to obtain an acceptable performance using the previous design criterion. The attempt in the previous section points out the difficulty in determining the messenger wire tension by simply reducing the reflection/amplification coefficient. Therefore, this section implements a neural

network-based optimisation approach to preliminarily investigate the potential of optimising the catenary parameters at the speed class of 400 km/h. Similar to the work in [36], the optimisation algorithm uses an artificial neural network coupled with a genetic algorithm [37] towards minimising the sum of squares of a vector-valued objective function. The training function for updating the weight and bias values of the neural network is the Bayesian Regularisation backpropagation [38]. In the training procedure of the neural network, the neural network is used as a virtual internal objective function equivalent to the objective function to reduce the contact force standard deviation of both leading and trailing pantographs. The genetic algorithm is used for minimising the output of the neural network.

Integrating the neural network-based optimisation algorithm into the finite element model of the pantograph-catenary system, the optimisation is performed to minimise the contact force standard deviation of the leading and trailing pantographs. The contact wire tension T_{cw}, messenger wire tension T_{mw} and stitch wire tension T_{sw} are taken as the optimised variables. The constraints are set as follows

$$\begin{aligned} &28.5\,\mathrm{kN} < T_{\mathrm{cw}} < 31.5\,\mathrm{kN};\\ &15\,\mathrm{kN} < T_{\mathrm{mw}} < 31.5\,\mathrm{kN};\\ &1\,\mathrm{kN} < T_{\mathrm{cw}} < 6\,\mathrm{kN} \end{aligned} \tag{13}$$

To ensure the same tension class, T_{cw} is only allowed to change $\pm 5\%$ with respect to the original value. A larger range is given for T_{mw} and T_{sw} to find the optimum solution for the interaction performance. As this is only a preliminary investigation, the geometric parameters of the catenary, like the dropper distribution and span length, are not included in the optimisation approach. Thus, the optimisation problem reads as follows:

$$\text{Objective: } \min\ \delta_{\mathrm{cf}}\left(T_{\mathrm{mw}}, T_{\mathrm{cw}}, T_{\mathrm{sw}}\right) \tag{14}$$

A normal Back-Propagation Neural Network (BPNN) is employed, which is a multi-layer feed-forward network consisting of multiple neurons . The BPNN algorithm minimizes the error between the network's output and the expected output, updating the weights and thresholds accordingly. The selection of the number of neurons in the hidden layer depends on the complexity of the problem. Insufficient hidden layer nodes may result in inadequate fitting ability for complex problems, while an excessive number of nodes can lead to overfitting. In this case, we have chosen to employ 200 BP neurons in the hidden layer. The neural network is used as a virtual internal objective function equivalent to the objective function as defined in Eq. (13), and the genetic algorithm is used for minimising the output of the neural network. The optimum solution of the neural network given by the genetic algorithm will be the optimum solution of Eq. (13) since the neural network and the objective function are equivalent. The optimised results of the contact force filtered within 0-25 Hz at 400 km/h are presented in Figure 11. It is seen that the optimisation approach can slightly reduce the contact force fluctuation of the leading pantograph while the performance of the trailing pantograph shows a significant improvement. The optimised variables are shown as follows:

Original	Optimised
T_{cw} = 30 kN	T_{cw} = 29.582 kN
T_{mw} = 21 kN	T_{mw} = 27.685 kN
T_{cw} = 3.5 kN	T_{cw} = 4.396 kN

After the optimisation, T_{cw} is slightly decreased, but T_{mw} and T_{sw} are significantly increased. Obviously, the optimisation results do not follow the previous design criteria, namely increasing T_{cw} and reducing T_{mw}, as the pantograph-catenary dynamics is very complicated and dependent on many coupling factors [39]. The comparison of contact force statistics between the original and optimised results is presented in Figure 12. It is seen that the optimisation approach is able to improve the interaction performance of both leading and trailing pantographs. The most significant improvement is manifested in the reduction of standard deviation by 19.72% and the increase of minimum value by 47.25 N of the trailing pantograph. A bigger improvement is expected when more variables, such as the catenary geometry and the pantograph parameters, are included in the optimisation.

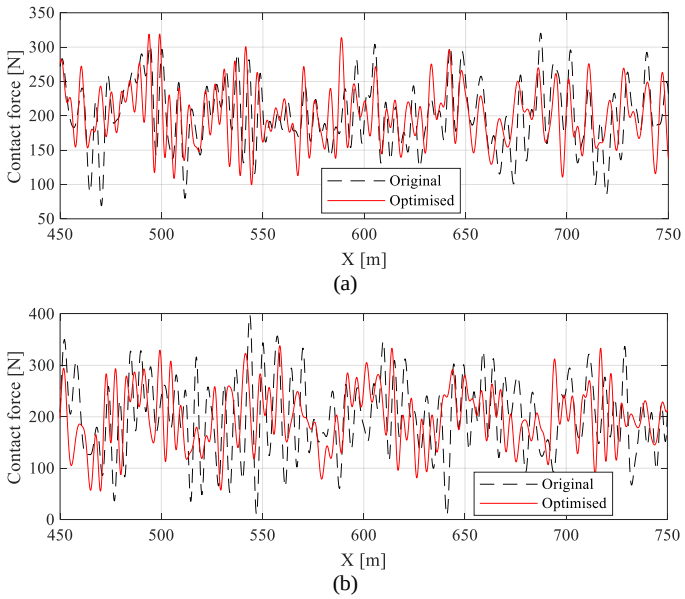

Figure 11. The optimised results of the contact force filtered within 0-25 Hz at 400 km/h: (a) Leading pantograph; (b) Trailing pantograph

The preliminary investigation in this section shows that the current collection quality exhibits a significant deterioration with the train speed approaching the wave propagation speed. The traditional specifications used for determining pantograph-catenary parameters do not work well for the speed of up to 400 km/h. Mainly, when the trailing pantograph is included, the simple reduction of the reflection wave coefficient cannot ensure a good current collection quality. It has been agreed by a number of scholars that the structural parameters have a very complicated effect on the high-speed performance, which cannot be accurately described in a simple equation. Even though some efforts can be made to make sense of the complex mechanism of structural parameters‘ effect, an optimisation approach is recommended

on the basis of a reliable numerical model to obtain the acceptable parameters' setting. This preliminary investigation indicates the possibility of achieving a significant improvement by adjusting some critical parameters. In the future, it is suggested that more parameters, or even the variability of span length, the unequal distribution of droppers among spans, the geometry in overlap sections, and the parameters of pantographs, can be included in the optimisation approach to achieve optimal global results. Collaboration with the rail operator is also essential to test the optimised results via field tests, which requires further investment and solid fundamental research output. The computational effort is also an important issue that should be optimised, and the potential of using surrogate models can be explored with the advancement of artificial intelligence technology.

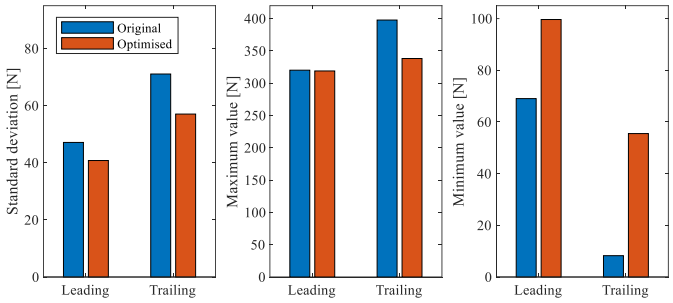

(a) (b) (c)

Figure 12. The comparison of the contact force statistics between original and optimised results at 400 km/h: (a) standard deviation; (b) maximum value, and (c) minimum value

5 Effect of Geometry Deviation

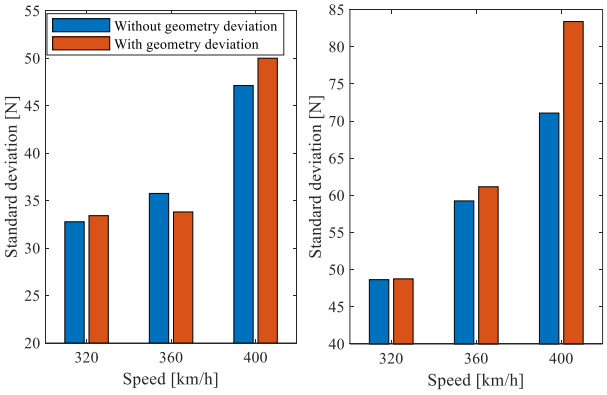

(a) (b)

Figure 13. The comparison of the contact force standard deviation between the original and distorted geometries at 400 km/h: (a) leading pantograph; (b) trailing pantograph

In this preliminary investigation, the PSD of the contact wire irregularities summarised in [40] is used to generate a series of contact wire irregularities. The initialisation of the catenary model is implemented to add the contact wire irregularities to the catenary configuration via the shape-finding method reported in [41]. The comparison of the resulting contact force standard deviation between the

original and distorted geometries is shown in Figure 13. It is obvious that the distorted geometry leads to a more significant increase in the contact force standard deviation with increasing speed. For the leading pantograph, the increment in the standard deviation increases from 1.98% at 320 km/h to 6.3% at 400 km/h. A more distinct effect can be seen on the trailing pantograph. The increment in the standard deviation increases from 0.23% at 320 km/h to 16.16% at 400 km/h.

The preliminary investigation points out a significant increase in the impact of geometry deviation on the interaction performance with the speed upgrade. It is expected the impact should be more sensitive if shorter-wavelength contact wire irregularities are considered. At 400 km/h and above, the detrimental wavelengths that cause serious deterioration of the current collection quality should be further identified. The improvement of the construction and maintenance standards for the railway catenary at 400 km/h and above are also necessary, and a more strict tolerance of contact wire distortion is allowed at this speed level.

5 Conclusions

Under the context of developing the next generation of high-speed railways for speeds of 400 km/h and above, this paper reviews the current research on pantograph-catenary interaction and proposes the perspectives for future studies to improve the performance of pantograph-catenary at the speed level of 400 km/h. The perspectives are summarised in the following aspects.

1) **Numerical model**: The current modelling technique is sufficient for modelling the pantograph-catenary system at the speed level of 380 km/h with acceptable numerical accuracy of reproducing the interaction behaviours within 0-20 Hz. More experimental data should be provided to validate the numerical model with more details, such as the overlap section and high-frequency behaviours at higher speeds. The necessity of including more details relevant to the high-frequency behaviours, such as the pantograph flexibility, short-wavelength wavelength, wear on the strip and contact wire and variability of parameters, should be further investigated.

2) **Assessment specification**: The current assessment standard specifies the frequency of interest for the contact force to be 0-20 Hz. The main frequency components will be outside of this specific frequency range with the increase of train speed up to 400 km/h and above. The increase of this frequency range requires the improvement of both the numerical and field test techniques. Combining with the maintenance demand, an appropriate frequency range of interest should be updated with the speed upgrade.

3) **Design specification**: The preliminary analysis indicates a distinct deterioration in the current collection quality with speed approaching the wave speed. The traditional measures of simply reducing the wave reflection coefficient used for determining catenary parameters do not work well for the speed of up to 400 km/h and above. The complexity of structural parameters' effect on high-speed performance that cannot be accurately described by a simple formula deserves further revelation. The optimisation approach is a feasible solution based on a reliable numerical model to obtain the acceptable parameters' setting. The computational effort is an important issue that deserves further attention.

4) **Geometry Deviation's Effect**: A tremendous increase in the geometry deviation's impact on the interaction performance can be observed with speed approaching the wave speed. At 400 km/h and above, the detrimental wavelengths that cause serious deterioration of the current collection quality should be further identified. The improvement of the construction and maintenance standards for the railway catenary at 400 km/h and above is also necessary, and a stricter tolerance of contact wire distortion deserves a deep discussion.

Acknowledgements

This work was supported in part by the National Natural Science Foundation of China (No, 52172408), Science and Technology Research and Development Project of China National Railway Group Co., Ltd (N2023T011-A(JB)), Research Project of China Academy of Railway Sciences Group Co., Ltd (2023YJ277)

References

[1] T. Smart and J. Irwin, "HS2 railway, UK – Route development to hybrid bill: Technical and operational requirements," *Proceedings of the Institution of Civil Engineers: Transport*, vol. 174, no. 1, pp. 25–32, Feb. 2021, doi: 10.1680/JTRAN.19.00062/ASSET/IMAGES/SMALL/JTRAN.19.00062-F3.GIF.

[2] F. Xu, "China High-Speed Railway: Country's Golden Name Card," *The Belt and Road*, pp. 3–17, 2018, doi: 10.1007/978-981-13-1105-5_1.

[3] N. Hashimoto, M. Sonobe, T. Kato, and T. Murakami, "Expanding response distance of position-corrective ground coil for speed increments in Shinkansen trains," *Transactions of the JSME (in Japanese)*, vol. 85, no. 878, pp. 19–00095, 2019, doi: 10.1299/TRANSJSME.19-00095.

[4] A. T. Burkov, L. S. Blazhko, and I. A. Ivanov, "Industrial technologies, mobility, and energy efficiency of electric traction of rail transport," *Russian Electrical Engineering*, vol. 87, no. 5, pp. 244–250, May 2016, doi: 10.3103/S1068371216050059/METRICS.

[5] Y. Sun, J. Xu, G. Lin, W. Ji, L. W.-I. T. on, and undefined 2020, "RBF neural network-based supervisor control for maglev vehicles on an elastic track with network time delay," *ieeexplore.ieee.orgY Sun, J Xu, G Lin, W Ji, L WangIEEE Transactions on Industrial Informatics, 2020•ieeexplore.ieee.org*, Accessed: Oct. 17, 2023. [Online]. Available: https://ieeexplore.ieee.org/abstract/document/9229504/

[6] Y. Sun, J. Xu, C. Chen, W. H.-I. T. on, and undefined 2022, "Reinforcement learning-based optimal tracking control for levitation system of maglev vehicle with input time delay," *ieeexplore.ieee.orgY Sun, J Xu, C Chen, W HuIEEE Transactions on Instrumentation and Measurement, 2022•ieeexplore.ieee.org*, Accessed: Oct. 17, 2023. [Online]. Available: https://ieeexplore.ieee.org/abstract/document/9693414/

[7] F. J. Smith, "Electric transmission for high-speed rail: A concept for a balanced-force pantograph and overhead contact system," *IEEE Vehicular*

Technology Magazine, vol. 13, no. 3, pp. 61–71, Sep. 2018, doi: 10.1109/MVT.2018.2848399.

[8] Z. Wang, Q. Zhou, F. Guo, A. Tang, X. Wang, and X. Chen, "Mathematical Model of Contact Resistance in Pantograph-Catenary System Considering Rough Surface Characteristics," *IEEE Transactions on Transportation Electrification*, vol. 8, no. 1, pp. 455–465, Mar. 2022, doi: 10.1109/TTE.2021.3095120.

[9] D. Feng, Q. Yu, X. Sun, H. Zhu, S. Lin, and J. Liang, "Risk Assessment for Electrified Railway Catenary System under Comprehensive Influence of Geographical and Meteorological Factors," *IEEE Transactions on Transportation Electrification*, vol. 7, no. 4, pp. 3137–3148, Dec. 2021, doi: 10.1109/TTE.2021.3078215.

[10] S. Bruni, G. Bucca, M. Carnevale, A. Collina, and A. Facchinetti, "Pantograph–catenary interaction: recent achievements and future research challenges," *International Journal of Rail Transportation*, vol. 6, no. 2, pp. 57–82, Apr. 2018, doi: 10.1080/23248378.2017.1400156.

[11] A. A. Shabana, "Definition of ANCF Finite Elements," *J Comput Nonlinear Dyn*, vol. 10, no. 5, 2015, doi: 10.1115/1.4030369.

[12] M. Berzeri and A. A. Shabana, "Development of simple models for the elastic forces in the absolute nodal co-ordinate formulation," *J Sound Vib*, vol. 235, no. 4, pp. 539–565, 2000, doi: 10.1006/jsvi.1999.2935.

[13] D. Zou, W. H. Zhang, R. P. Li, N. Zhou, and G. M. Mei, "Determining damping characteristics of railway-overhead-wire system for finite-element analysis," *Vehicle System Dynamics*, vol. 54, no. 7, pp. 902–917, 2016, doi: 10.1080/00423114.2016.1172715.

[14] O. Lopez-Garcia, A. Carnicero, and J. L. Maroño, "Influence of stiffness and contact modelling on catenary-pantograph system dynamics," *J Sound Vib*, vol. 299, no. 4–5, pp. 806–821, 2007, doi: 10.1016/j.jsv.2006.07.018.

[15] W. J. Qian, G. X. Chen, W. H. Zhang, H. Ouyang, and Z. R. Zhou, "Friction-induced, self-excited vibration of a pantograph-catenary system," *Journal of Vibration and Acoustics, Transactions of the ASME*, vol. 135, no. 5, p. 051021, 2013, doi: 10.1115/1.4023999.

[16] Y. Song, A. Rønnquist, and P. Nåvik, "Assessment of the high-frequency response in railway pantograph-catenary interaction based on numerical simulation," *IEEE Trans Veh Technol*, vol. 69, no. 10, pp. 10596–10605, 2020, doi: 10.1109/TVT.2020.3015044.

[17] M. Busch and B. Schweizer, "Coupled simulation of multibody and finite element systems: An efficient and robust semi-implicit coupling approach," *Archive of Applied Mechanics*, vol. 82, no. 6, pp. 723–741, Jun. 2012, doi: 10.1007/S00419-011-0586-0/METRICS.

[18] Y. Ye, P. Huang, Y. Sun, and D. Shi, "MBSNet: A deep learning model for multibody dynamics simulation and its application to a vehicle-track system," *Mech Syst Signal Process*, vol. 157, p. 107716, Aug. 2021, doi: 10.1016/j.ymssp.2021.107716.

[19] European Committee for Electrotechnical Standardization, *EN 50367. Railway applications — Current collection systems — Technical criteria for the*

interaction between pantograph and overhead line. Brussels: European Standards (EN), 2016.

[20] S. Kusumi, T. Fukutani, and K. Nezu, "Diagnosis of Overhead Contact Line based on Contact Force," *Quarterly Report of RTRI*, vol. 47, no. 1, pp. 39–45, Feb. 2006, doi: 10.2219/RTRIQR.47.39.

[21] J. Pombo and P. Antunes, "A Comparative Study between Two Pantographs in Multiple Pantograph High-Speed Operations," *International Journal of Railway Technology*, vol. 2, no. 1, pp. 83–108, 2013, doi: 10.4203/ijrt.2.1.4.

[22] J. Pombo and J. Ambrsio, "Multiple pantograph interaction with catenaries in high-speed trains," *J Comput Nonlinear Dyn*, vol. 7, no. 4, p. 041008, Oct. 2012, doi: 10.1115/1.4006734.

[23] Z. Xu, Y. Song, and Z. Liu, "Effective measures to improve current collection quality for double pantographs and catenary based on wave propagation analysis," *IEEE Trans Veh Technol*, vol. 69, no. 6, pp. 6299–6309, 2020, doi: 10.1109/TVT.2020.2985382.

[24] L. Cheng, T. Wang, and Y. Wang, "A novel fault location method for distribution networks with distributed generations based on the time matrix of traveling-waves," *Protection and Control of Modern Power Systems*, vol. 7, no. 1, pp. 1–11, Dec. 2022, doi: 10.1186/S41601-022-00265-8/TABLES/6.

[25] J. F. Doyle, "Wave Propagation in Structures," *Wave Propagation in Structures*, pp. 126–156, 1989, doi: 10.1007/978-1-4684-0344-2_6.

[26] A. v. Metrikine and M. v. Tochilin, "STEADY-STATE VIBRATIONS OF AN ELASTIC RING UNDER A MOVING LOAD," *J Sound Vib*, vol. 232, no. 3, pp. 511–524, May 2000, doi: 10.1006/JSVI.1999.2756.

[27] Y. Song, Z. Liu, F. Duan, Z. Xu, and X. Lu, "Wave propagation analysis in high-speed railway catenary system subjected to a moving pantograph," *Appl Math Model*, vol. 59, pp. 20–38, 2018, doi: 10.1016/j.apm.2018.01.001.

[28] A. V. Metrikine and A. L. Bosch, "Dynamic response of a two-level catenary to a moving load," *J Sound Vib*, vol. 292, no. 3–5, pp. 676–693, 2006, doi: 10.1016/j.jsv.2005.08.026.

[29] F. Kiessling, R. Puschmann, A. Schmieder, and E. Schneider, *Contact lines for electric railways, third edition*, Third Edit., vol. 116, no. 3. John Wiley & Sons, 2018.

[30] J. Zhang, W. Liu, and Z. Zhang, "Sensitivity analysis and research on optimisation methods of design parameters of high-speed railway catenary," *IET Electrical Systems in Transportation*, vol. 9, no. 3, pp. 150–156, Sep. 2019, doi: 10.1049/iet-est.2018.5007.

[31] K. Lee, Y. H. Cho, S. Y. Kwon, and Y. Park, "A study on a sensitivity analysis of design parameters for the speed-up of overhead rigid conductor system," *Transactions of the Korean Institute of Electrical Engineers*, vol. 66, no. 2, pp. 453–458, 2017, doi: 10.5370/KIEE.2017.66.2.453.

[32] R. J. Paul and T. S. Chanev, "Simulation optimisation using a genetic algorithm," 1998.

[33] S. Gregori, M. Tur, E. Nadal, and F. J. Fuenmayor, "An approach to geometric optimisation of railway catenaries," *Vehicle System Dynamics*, vol. 56, no. 8, pp. 1162–1186, Aug. 2018, doi: 10.1080/00423114.2017.1407434.

[34] J. Ambrósio, J. Pombo, and M. Pereira, “Optimization of high-speed railway pantographs for improving pantograph-catenary contact,” *Theoretical and Applied Mechanics Letters*, vol. 3, no. 1, p. 013006, 2013, doi: 10.1063/2.1301306.

[35] J. H. Lee, Y. G. Kim, J. S. Paik, and T. W. Park, “Performance evaluation and design optimization using differential evolutionary algorithm of the pantograph for the high-speed train,” *Journal of Mechanical Science and Technology*, vol. 26, no. 10, pp. 3253–3260, Oct. 2012, doi: 10.1007/s12206-012-0833-5.

[36] K. Su, J. Zhang, J. Zhang, T. Yan, and G. Mei, “Optimisation of current collection quality of high-speed pantograph-catenary system using the combination of artificial neural network and genetic algorithm,” *Vehicle System Dynamics*, 2022, doi: 10.1080/00423114.2022.2045029.

[37] M. Kolat, T. Tettamanti, T. Bécsi, and D. Esztergár-Kiss, “On the relationship between the activity at point of interests and road traffic,” *Communications in Transportation Research*, vol. 3, p. 100102, Dec. 2023, doi: 10.1016/J.COMMTR.2023.100102.

[38] D. J. C. MacKay, “A Practical Bayesian Framework for Backpropagation Networks,” *Neural Comput*, vol. 4, no. 3, pp. 448–472, May 1992, doi: 10.1162/NECO.1992.4.3.448.

[39] Y. Song, F. Duan, and Z. Liu, “Analysis of Critical Speed for High-Speed Railway Pantograph-Catenary System,” *IEEE Trans Veh Technol*, vol. 71, no. 4, pp. 3547–3555, 2022, doi: 10.1109/TVT.2021.3136920.

[40] Y. Song, F. Duan, F. Wu, Z. Liu, and S. Gao, “Assessment of the Current Collection Quality of Pantograph-Catenary with Contact Line Height Variability in Electric Railways,” *IEEE Transactions on Transportation Electrification*, vol. 7782, no. c, pp. 1–1, 2021, doi: 10.1109/tte.2021.3090477.

[41] Y. Song, T. Jiang, P. Nåvik, and A. Rønnquist, “Geometry deviation effects of railway catenaries on pantograph–catenary interaction: a case study in Norwegian Railway System,” *Railway Engineering Science*, pp. 1–12, Aug. 2021, doi: 10.1007/s40534-021-00251-0.